# Backbone Dynamics of (Pro-Hyp-Gly)$_{10}$ and a Designed Collagen-like Triple-Helical Peptide by $^{15}$N NMR Relaxation and Hydrogen-Exchange Measurements[†,1]

Pei Fan,[‡] Ming-Hua Li,[‡] Barbara Brodsky,[§] and Jean Baum*[,‡]

*Department of Chemistry, Rutgers University, Piscataway, New Jersey 08855-0939, and Department of Biochemistry, UMDNJ-Robert Wood Johnson Medical School, Piscataway, New Jersey 08854*

*Received July 15, 1993; Revised Manuscript Received September 8, 1993*[⊗]

ABSTRACT: The backbone dynamics of specific residues in two collagen-like triple-helical peptides with (X-Y-Gly)$_n$ sequences have been investigated using two-dimensional inverse-detected $^{15}$N NMR relaxation measurements and hydrogen-exchange experiments. One peptide, (POG)$_{10}$, has the highest possible imino acid content and is considered to be a very stable prototype of a triple helix. The second peptide, (POG)$_3$ITGARGLAGPOG(POG)$_3$ (denoted T3-785), models an imino acid poor region of type III collagen and contains 12 residues from near the unique collagenase cleavage site. $^{15}$N relaxation parameters and hydrogen-exchange data were obtained for a glycine residue in the center of (POG)$_{10}$ and for the tripeptide unit Gly-Leu-Ala in the middle of T3-785. Analysis of the relaxation data of the rodlike triple-helical peptides required the assumption of anisotropic overall motion, and the model-free approach of Lipari and Szabo (1982) was used to derive overall motional parameters and the order parameter, $S^2$, that describes the amplitudes of the internal motion. First the mobilities of the Gly, Leu, and Ala residues in peptide T3-785 were compared. Both hydrogen-exchange methods and relaxation measurements indicated that the residue in the Y position (Ala) is more mobile than residues in the Gly and X positions (Leu). The slower exchange rates of Gly and Leu compared to that of Ala are consistent with the two-hydrogen-bonded model for the triple helix. Then the backbone mobilities of the central Gly residue were compared for the two peptides (POG)$_{10}$ and T3-785. In this case, $^{15}$N relaxation measurements give different results from hydrogen exchange. The glycine residues in the trimer form of both T3-785 and (POG)$_{10}$ have high values for the order parameter (near 0.85), suggesting similar small-amplitude internal motions and rigid backbones in both peptides. In contrast to the similar values of the order parameters, hydrogen-exchange data indicate that the central Gly exchanges at a faster rate in the trimer form of T3-785 than in (POG)$_{10}$. These results suggest that a Gly in the imino acid rich environment of (POG)$_{10}$ is dynamically different from a Gly in the imino acid poor environment of T3-785 and that the difference lies in the slower motion related to stability, rather than the faster motion on the picosecond time scale. This sequence-dependent difference in dynamical properties may have important consequences for recognition processes in collagen.

The triple-helical conformation is one of the basic protein structural motifs, forming the major repeating unit in collagen and a rodlike domain in a number of other proteins, such as the macrophage scavenger receptor (Kodama et al., 1990) and C1q (Brodsky-Doyle et al., 1976). There are strict sequence constraints required to generate the triple-helical conformation. Every third residue must be glycine, and a high proportion of the residues must be the imino acids proline and hydroxyproline (Fraser & MacRae, 1973; Fietzek & Kuhn, 1975). The molecular conformation of the triple helix was deduced from fiber diffraction studies on collagen, together with sequence and composition data (Rich & Crick, 1961; Ramachandran, 1967). In one molecule, there are three polypeptide chains, each in an extended polyproline II like helix. These chains are staggered by one residue with respect to each other and twisted around a common axis, to give a supercoiled structure. A high imino acid content is required to maintain the extended-chain conformation (Nemethy & Scherage, 1984), and the close packing of the three chains restricts every third residue to be a glycine, generating a (X-Y-Gly)$_n$ repeating pattern. There are hydrogen bonds between the peptide groups in different chains. The best available model, representing a linked-atom least-squares refinement of the fiber diffraction data (Fraser et al., 1979), is a refined version of the collagen structure proposed by Rich and Crick (1961) and contains one hydrogen bond between the NH of the Gly residue and the C=O of the residue in the X position (Figure 1).

The rodlike triple-helical domains of collagen associate to form fibrils and higher order structures found in connective tissues (van der Rest & Garrone, 1991; Linsenmayer, 1991). The most well characterized collagens are the fibril-forming family which are present in fibrils with an axial period of $D$ = 67 nm. Members of this family include type I collagen, a heterotrimer, found in tendon and bone, and type III collagen, a homotrimer, found together with type I in skin and blood vessels (van der Rest & Garrone, 1991; Linsenmayer, 1991).

[†] This work was supported by the Searle Scholar Fund/Chicago Community Trust (J.B.), a Biomedical Research Support Grant under the Department of Public Health Science (J.B.), and NIH Grants GM45302 (J.B.) and AR19626 (B.B.).

* To whom correspondence should be addressed.

[‡] Rutgers University.

[§] UMDMJ-Robert Wood Johnson Medical School.

[⊗] Abstract published in *Advance ACS Abstracts*, November 15, 1993.

[1] Abbreviations: NMR, nuclear magnetic resonance; 1D, one-dimensional; 2D, two-dimensional; CD, circular dichroism; NOE, nuclear Overhauser enhancement; HMQC, $^1$H-detected heteronuclear multiple quantum coherence spectroscopy; Hyp, hydroxyproline; standard three letter codes and one letter codes are used for amino acids; one letter code O is used for hydroxyproline.

0006-2960/93/0432-13299$04.00/0 

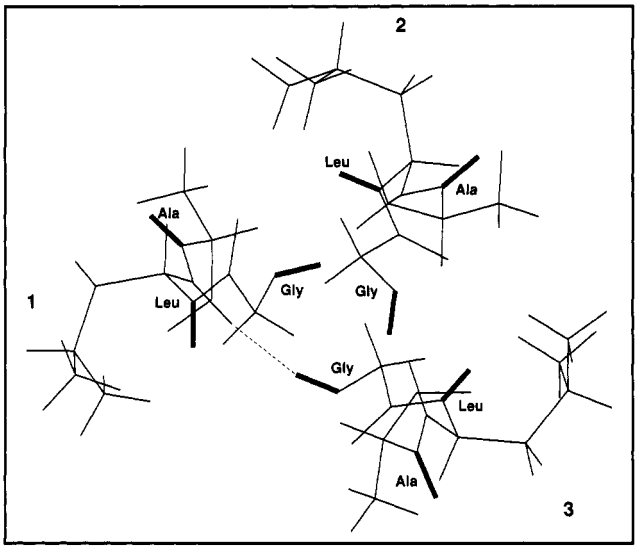


FIGURE 1: Cross section of the triple-helical structure. One tripeptide unit Gly-Leu-Ala from each chain of T3-785 is shown. The amide protons of each residue are highlighted with a heavy line. A hydrogen bond between the amide proton of the Gly in chain 3 and the carbonyl oxygen of the Leu in chain 1 is shown with a dashed line. The amide protons of the other two Gly residues in chains 1 and 2 are also hydrogen-bonded to the carbonyl oxygen of residues in the X position in the adjacent tripeptide unit. The computer model of T3-785 is generated from the model of $(POG)_{10}$, obtained from the X-ray fiber diffraction data (Fraser et al., 1979), by replacing the central nine residues with the residues Ile-Thr-Gly-Ala-Arg-Gly-Leu-Ala-Gly, and energy-minimized with IMPACT (Kitchen et al., 1990) using steepest descent and conjugated gradient algorithms.

In addition to forming the structural basis of collagen, certain sequences in the triple helix may be specifically recognized by other molecules, for example integrin receptors on cells and other extracellular matrix molecules such as fibronectin (Guidry et al., 1990; Kirchhofer et al., 1990; Staatz et al., 1991). It has been suggested that triple-helical regions with a relatively low imino acid content may be involved in these recognition sites. An example is the unique vertebrate collagenase cleavage site of types I, II, and III collagens, which is flanked on the C-terminal side by 12 X-Y-Gly residues with no imino acids (Fields, 1991). Imino acid poor regions may be recognizable because of differences in the triple-helical conformation, which could lead to the formation of two hydrogen bonds per tripeptide (Ramachandran, 1967; Fraser & MacRae, 1973), or because of increased flexibility (Miller, 1984; Dolz & Heidermann, 1986). The possibility has also been raised that such regions could loop out from the triple helix (Ryhanen et al., 1983; Fields, 1991).

One of the properties that could play a role in specific recognition of different regions of the triple helix is molecular motion. Flexibility may vary along the 1000-residue collagen triple helix and could be influenced by local concentrations of imino acids as well as specific X and Y residues. Quantification of motional variations can be approached by solution and solid-state NMR dynamics studies such as relaxation measurements, line shape analysis, and hydrogen exchange. Deuterium and $^{13}C$ relaxation measurements and line shape analysis of collagen with labeled amino acids have demonstrated the mobility of the collagen molecules both in solution and in fibrils (Jelinski & Torchia, 1980; Jelinski et al., 1980; Torchia, 1982). Studies were also done to characterize the mobility of a triple-helical collagen cyanogen bromide fragment, $\alpha 1$(I)-CB2, and indicated that the overall motion of the trimer was anisotropic (Torchia et al., 1975). Numerous hydrogen-exchange studies have been carried out on collagen, as well as on triple-helical peptides, using tritium exchange and NMR (von Hippel, 1967; Segal, 1969; Katz, 1970; Privalov et al., 1979). The fraction of slowly exchanging hydrogens, which represent an average of all the amides in the molecules, was used to infer the number of hydrogen bonds in the triple helix.

Peptides which satisfy the stringent $(X\text{-}Y\text{-}Gly)_n$ sequence requirement and have a high imino acid content will form stable triple helices in aqueous solution and can be used to model different regions of a collagen chain. We have studied the conformation of two triple-helical peptides by NMR to examine the effects of different amino acid sequences in the X and Y positions of the $(X\text{-}Y\text{-}Gly)_n$ repeat. The peptide $(POG)_{10}$, a trimer with high stability, is a model for imino acid rich regions of collagen, such as the repeating Pro-Hyp-Gly triplets found at the C-terminal ends of most fibrillar collagen chains (Fietzek & Kuhn, 1975). The peptide $(POG)_3$ITGARGLAGPOG$(POG)_3$, denoted T3-785, was designed with 12 X-Y-Gly residues from type III collagen and models a biologically important imino acid poor region of collagen. The 12 residues are located near the collagenase cleavage site (Seyer et al., 1980; Fields, 1991) and contain the single trypsin cleavage site (RG) in native type III collagen (Miller et al., 1976). In addition, the sequence contains the site of a Gly to Ser amino acid substitution that results in Ehlers Danlos Syndrome Type IV (Tromp et al., 1989). The 12 residues from type III are surrounded by $(POG)_3$ caps to provide stability. Two-dimensional NMR studies on $(POG)_{10}$ have shown that the conformation in solution is similar to the fiber diffraction model (Li et al., 1993). Studies on the trimeric peptide T3-785, using 2D NMR, have allowed assignments of a specific triplet Gly-Leu-Ala in all three chains. NOEs between residues in different chains provide definitive evidence for a one-residue stagger between three parallel chains and are consistent with the Pro-Hyp-Gly triple-helix model even in this imino acid lacking region (Li et al., 1993).

In addition to obtaining dynamics information by hydrogen exchange (Woodward & Hilton, 1979; Wagner, 1983; Englander & Kallenbach, 1984), recently, 2D inverse-detected heteronuclear NMR relaxation measurements have been applied to globular proteins to obtain information about fast backbone dynamics at the individual residue level (Nirmala & Wagner, 1988; Kay et al., 1989; Clore et al., 1990; Palmer et al., 1991; Schneider et al., 1992; Stone et al., 1992; Kordel et al., 1992; Barbato et al., 1992; Powers et al., 1992; Redfield et al., 1992; Berglund et al., 1992; Stone et al., 1993; Constantine et al., 1993). In this paper, we present $^{15}N$ relaxation and hydrogen–deuterium exchange studies on specific residues in the two triple-helical peptides $(POG)_{10}$ and T3-785 to obtain information about the motion of individual backbone amides. Relaxation measurements are analyzed using the model-free formalism of Lipari and Szabo (1982) to obtain internal motional parameters. In triple-helical peptides, the rodlike dimensions of the peptides (Fraser et al., 1979) and results of previous NMR studies (Torchia et al., 1975; Li et al., 1993) dictate the use of anisotropic overall motion in the analysis of the relaxation data. This is distinct from the analysis of globular proteins, where overall motion is usually assumed to be isotropic (Kay et al., 1989; Clore et al., 1990; Palmer et al., 1991), although the possibility of anisotropic motion was recently considered (Barbato et al., 1992; Schneider et al., 1992; Berglund et al., 1992). The present $^{15}N$ dynamics studies are carried out on one glycine residue in the middle of $(POG)_{10}$ and on a tripeptide unit Gly-Leu-Ala in the middle of T3-785.

Dynamics studies on these residues, which represent very different kinds of X-Y-Gly sequences in collagen, allow determination of their sequence-dependent motional properties and hydrogen-exchange rates. The complementary information about motions on the different time scales obtained by hydrogen-exchange and $^{15}N$ relaxation measurements may clarify whether flexibility and stability are important in specifying functional regions along a triple-helical molecule.

## MATERIALS AND METHODS

*Peptides.* The triple-helical peptides (Pro-Hyp-Gly)$_4$Pro-Hyp-Gly*(Pro-Hyp-Gly)$_5$ and (Pro-Hyp-Gly)$_3$Ile-Thr-Gly-Ala-Arg-Gly*-Leu*-Ala*-Gly-Pro-Hyp-Gly(Pro-Hyp-Gly)$_3$ (T3-785) were synthesized and purified by the CABM Microchemistry Laboratory (Rutgers University/UMDNJ, Piscataway, NJ) as previously described (Li et al., 1993). Selective $^{15}N$ labeling was achieved by using commercially available $^{15}N$-labeled amino acids during the synthesis, and the residues with an asterisk are labeled with a $^{15}N$ isotope. Mass spectrometry confirmed the identity of the peptides, and HPLC indicated a high degree of purity (>95%).

*NMR Spectroscopy.* For the NMR experiments, the model peptide (Pro-Hyp-Gly)$_{10}$ was dissolved in 90% $H_2O$/10% $D_2O$ solution with 0.1 M deuterated acetic acid; T3-785 peptide was dissolved in 90% $H_2O$/10% $D_2O$ solution. The concentrations of both peptides were ~4 mM trimer. NMR experiments were carried out on a Varian VXR-500 spectrometer at 10 °C. $^{15}N$ $T_1$ and $T_2$ and heteronuclear NOE were measured using experiments with "reverse" proton detection (Kay et al., 1989, 1992). The pulse sequences designed to remove cross-correlation between the dipolar and chemical shift anisotropy relaxation processes during the $T_1$ and $T_2$ relaxation times were used (Kay et al., 1992; Palmer et al., 1992).

For the peptide (Pro-Hyp-Gly)$_{10}$, 1D versions of the pulse sequences were used since only one amide resonance is observed in the spectrum (Kay et al., 1989, 1992). The experiments were carried out with a spectral width of 5000 Hz and 2048 real data points, 1024 scans were accumulated for each experiment, a delay time of 2.8 s was used between each scan, and water suppression was achieved using low-power presaturation for 1.2 s before the first pulse. $T_1$ values were measured with 10 relaxation delays of 20, 60, 120, 180, 241, 301, 401, 501, 601, and 722 ms. For $T_2$ measurements, 10 relaxation delays were used with 6, 12, 18, 24, 30, 42, 54, 66, 78, and 90 ms. The $T_1$ and $T_2$ relaxation experiments were repeated three times to obtain an error estimate. To measure the $^1H$-$^{15}N$ NOEs, two spectra were recorded with and without proton saturation. Proton saturation was obtained by using 120° pulses spaced at 20-ms intervals for 3 s prior to the first $^{15}N$ 90° pulse (Kay et al., 1989). The NOE experiments were repeated three times.

For the peptide T3-785, 2D versions of the pulse sequences were used to measure the relaxation processes (Kay et al., 1989, 1992). A spectral width of 5000 Hz was used in the t2 dimension, and a sweep width of 1000 Hz was used in the t1 dimension. Quadrature detection in the t1 dimension was achieved by using the time-proportional phase incrementation (TPPI) method (Redfield & Kunz, 1975; Marion & Wuthrich, 1983). 2D data sets with 2K data points and 200 t1 increments were recorded. For the $T_1$ and $T_2$ experiments, 32 scans per t1 increment were accumulated. For the NOE experiment, 128 scans per t1 increment were recorded. $T_1$ values were obtained with eight relaxation delays of 20, 100, 200, 320, 450, 600, 750, and 900 ms, and $T_2$ values were measured with delays of 6, 18, 30, 48, 66, 84, 108, and 120 ms. For measuring $^1H$-$^{15}N$ NOE, spectra were recorded in the presence and absence of $^1H$ saturation, and the proton saturation was carried out the same way as in the 1D experiment. Both $T_1$ and $T_2$ experiments were performed three times, and the NOE experiment was performed two times. For the $T_1$ and $T_2$ experiments, two data sets showed very similar $T_1$ and $T_2$ values but the third data set showed a systematic increase in the $T_2$ values relative to the other two, although all the trends within a given data set were similar. A one-way analysis of variance with repeated measures (Cody & Smith, 1987) was carried out to test the null hypothesis that the three data sets are indistinguishable, and this hypothesis was rejected at a $P < 0.05$ level. The Duncan multiple range test (Cody & Smith, 1987) indicated the first two data sets were indistinguishable ($P < 0.05$) while the third data set was different from the other two. On this basis, we have excluded the third data set.

The amide hydrogen exchange studies for each of the labeled residues in (POG)$_{10}$ and T3-785 were carried out using $^1H$-$^{15}N$ HMQC experiments (Mueller, 1979; Bax et al., 1983) at 10 °C, pH 3.6. The samples were quickly dissolved in $D_2O$ to initiate the exchange, and HMQC spectra were taken at different time intervals. The spectral widths in the t2 and t1 dimensions were the same as in the relaxation measurements. 2K data points in the t2 dimension and 96 t1 increments were recorded. To study the monomer exchange, two scans per t1 increment were accumulated, resulting in an acquisition of 4.2 min for a 2D spectrum. For the trimer exchange, eight scans per t1 increment were accumulated, resulting in an acquisition time of 16.8 min. The rates of exchange were obtained by monitoring the decrease of peak heights in the HMQC spectra as a function of time, and the decay curves were fit to single exponentials.

All data were processed using the software FELIX version 2.0 (Hare Research, Inc.) on a Silicon Graphics INDIGO workstation. For the 2D data sets, 90° phase shifted sinebell window functions were applied in both dimensions prior to Fourier transformation. The final 2D spectra were zero-filled to 4K × 4K real data points. To obtain the relaxation times $T_1$ and $T_2$, the peak height for each individual residue was monitored as a function of relaxation delay, and the resultant decay curves were fit to single exponentials. The NOE was calculated from the ratio of the peak heights in the correlation spectra collected with and without proton saturation.

## THEORETICAL TREATMENT OF RODLIKE ANISOTROPIC PEPTIDES

An anisotropic treatment of overall motion needs to be used to analyze the relaxation parameters of triple-helical peptides. A molecular model of (POG)$_{10}$, based on the fiber diffraction data, shows that the peptide has a rod shape with a length of 93 Å and a diameter of 10–15 Å (Fraser et al., 1979), and the structure in solution is not very different from this model (Li et al., 1993) (Figure 2). In addition, 1D NMR relaxation measurements on the peptide $\alpha$1(I)-CB2, a 36-residue CNBr peptide from the $\alpha$1 chain of type I collagen, have indicated that the motion of the molecule is anisotropic (Torchia et al., 1975).

The relaxation parameters $T_1$ and $T_2$ and NOE enhancement of the amide $^{15}N$ nucleus are caused mainly by the dipolar interaction with its directly bonded proton and by the $^{15}N$ chemical shift anisotropy. The equations for the relaxation rates ($R_1 = 1/T_1$, $R_2 = 1/T_2$) and the NOE enhancement are given by (Abragam, 1961)

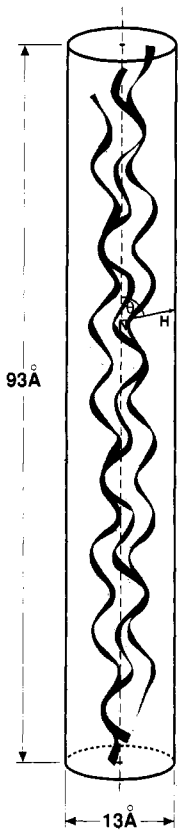


FIGURE 2: Schematic diagram of the triple-helical peptide represented as a cylinder. The dimensions of the molecule obtained from the fiber diffraction data are indicated. A representative N–H vector and the angle between the vector and the helix axis ($\theta$) are also illustrated. The backbone ribbon diagram of the model triple-helical peptide $(POG)_{10}$ is shown with the cylinder.

$$R_1 = \frac{\hbar^2\gamma_N^2\gamma_H^2}{4r_{NH}^6}[J(\omega_H - \omega_N) + 3J(\omega_N) + 6J(\omega_H + \omega_N)] + \frac{\omega_N^2(\delta_\parallel - \delta_\perp)^2}{3}J(\omega_N) \quad (1)$$

$$R_2 = \frac{\hbar^2\gamma_N^2\gamma_H^2}{8r_{NH}^6}[4J(0) + J(\omega_H - \omega_N) + 3J(\omega_N) + 6J(\omega_H) + 6J(\omega_H + \omega_N)] + \frac{\omega_N^2(\delta_\parallel - \delta_\perp)^2}{18}[3J(\omega_N) + 4J(0)] + R_{ex} \quad (2)$$

$$\text{NOE} = 1 + \frac{\gamma_H}{\gamma_N}\left(\frac{\hbar^2\gamma_N^2\gamma_H^2}{4r_{NH}^6}\right)\frac{6J(\omega_H + \omega_N) - J(\omega_H - \omega_N)}{R_1} \quad (3)$$

where $\hbar$ is Planck's constant divided by $2\pi$; $\gamma_H$ and $\gamma_N$ are the gyromagnetic ratios for the amide proton and the $^{15}N$ nuclei, respectively; $r_{NH}$ is the N–H bond length; $\omega_H$ and $\omega_N$ are the Larmor frequencies for the $^1H$ and $^{15}N$ nuclei, respectively; $\delta_\parallel$ and $\delta_\perp$ are the parallel and perpendicular components of the chemical shift tensor; $J(\omega_i)$ is the spectral density function; and $R_{ex}$ is the contribution of chemical exchange processes to the $T_2$ relaxation.

The information about the molecular motion is contained in the spectral density function, which is the Fourier transform of the rotational correlation function of the macromolecule. For globular proteins, the overall motion is often assumed to be isotropic and the total correlation function can be factored into the product of overall motion and internal motion. Using the model-free formalism proposed by Lipari and Szabo (1982), the spectral density function for isotropic overall motion can be written as

$$J(\omega) = \frac{2}{5}\left[\frac{S^2\tau_c}{1 + (\omega\tau_c)^2} + \frac{(1 - S^2)\tau}{1 + (\omega\tau)^2}\right] \quad (4)$$

where $S^2$ is the generalized order parameter, which reflects the spatial restriction of the N–H bond vector, $\tau_c$ is the overall rotational correlation time, $1/\tau = 1/\tau_c + 1/\tau_e$, and $\tau_e$ is the effective correlation time for the internal motion.

For anisotropic motion which is required in the case of triple-helical peptides, the total correlation function is formally no longer the product of the correlation function of the overall motion and the internal motion. However, the approximation can still be made, especially when the internal motion is in the extreme narrowing limit (Lipari & Szabo, 1982). Using the spectral density for an axially symmetric molecule (Woessner, 1962), and assuming that the internal motion is much faster than the overall motion ($\tau_e \ll \tau_1, \tau_2, \tau_3$) and that the internal motion is in the extreme narrowing limit ($(\omega\tau_e)^2 \ll 1$), the total spectral density function can be approximated by

$$J(\omega) = \frac{2}{5}\left[S^2\left(\frac{A\tau_1}{1 + (\omega\tau_1)^2} + \frac{B\tau_2}{1 + (\omega\tau_2)^2} + \frac{C\tau_3}{1 + (\omega\tau_3)^2}\right) + (1 - S^2)\tau_e\right] \quad (5)$$

with

$$A = \frac{1}{4}(1 - 3\cos^2\theta)^2$$

$$B = 3\sin^2\theta\cos^2\theta$$

$$C = \frac{3}{4}\sin^4\theta$$

where $\theta$ is the angle between the N–H vector and the long symmetry axis of the molecule. The three correlation times are a function of the rotational diffusion constants perpendicular ($D_\perp$) and parallel ($D_\parallel$) to the long molecular axis:

$$1/\tau_1 = 6D_\perp$$

$$1/\tau_2 = 5D_\perp + D_\parallel$$

$$1/\tau_3 = 2D_\perp + 4D_\parallel$$

At a given temperature, the definitions of $D_\perp$ and $D_\parallel$ depend on the model and dimensions that describe the anisotropic molecule. Previously, in the analysis of relaxation data, an ellipsoid model was used to describe a triple-helical peptide in solution (Torchia et al., 1975). NMR solution studies of $(POG)_{10}$ and T3-785 indicate that the central region of the peptide is similar to the helix derived from fiber diffraction studies and that the ends are less ordered (Li et al., 1993). These data support the use of a cylindrical model rather than an ellipsoid in the analysis of $(POG)_{10}$ and T3-785. For a cylinder of length $L$ and a diameter $b$, the rotational diffusion constants in a solution at temperature $T$ with viscosity $\eta$ are given by the following equations (Lamb, 1945; Broersma, 1960):

$$D_{\parallel} = k_B T/\pi\eta b^2 L \quad (6)$$

$$D_{\perp} = (3k_B T/\pi\eta L^3)\{\ln(2L/b) - 1.57 + 7[1/\ln(2L/b) - 0.28]^2\} \quad (7)$$

where $k_B$ is the Boltzmann constant. In the case where $\tau_e$, the effective correlation time, is too small to contribute to the spectral density function ($\tau_e \rightarrow 0$), eq 5 reduces to

$$J(\omega) = \frac{2}{5}S^2\left(\frac{A\tau_1}{1 + (\omega\tau_1)^2} + \frac{B\tau_2}{1 + (\omega\tau_2)^2} + \frac{C\tau_3}{1 + (\omega\tau_3)^2}\right) \quad (8)$$

To analyze $T_1$, $T_2$, and NOE relaxation data, it is important to choose the appropriate form of the spectral density function and to determine whether conformational averaging is making a significant contribution to the $T_2$ relaxation. For isotropic globular proteins, a set of procedures have been formulated (Clore et al., 1990; Palmer et al., 1991). In general, the choice of the spectral density function and the use of the exchange term $R_{ex}$ in the $T_2$ relaxation depend on the deviation of the $R_2/R_1$ ratio from the mean and on the value of the experimental NOE. The basis of the developed procedures derive from the fact, that in the fast internal motion limit and the absence of chemical exchange, the $R_2/R_1$ ratio is only a function of the overall correlation time and, therefore, should be a constant from residue to residue (Kay et al., 1989; Clore et al., 1990). Therefore in isotropic globular proteins, when the $R_2/R_1$ ratio is not a constant or deviates by one standard deviation from the mean, the interpretation is that the contribution from $\tau_e$ cannot be neglected and/or that an exchange term is required.

The procedures that have been developed for isotropic molecules cannot readily be applied to rodlike molecules such as triple-helical peptides. In the case of anisotropic overall motion, even in the absence of chemical exchange and negligible contribution from $\tau_e$, the $R_2/R_1$ ratio is not expected to be a constant from residue to residue but rather depends on the angle $\theta$ that the N–H vector makes with the long axis of the molecule (Barbato et al., 1992) (Figure 2). Therefore deviation of the $R_2/R_1$ ratio from the mean is no longer a meaningful measure for choosing the spectral density function or deciding whether to include $R_{ex}$ in the $T_2$ relaxation.

The second criterion applied to globular proteins in choosing the form of the spectral density function is to consider the magnitude of the NOE, which is sensitive to the effective correlation time of the internal motion $\tau_e$. When the experimental NOE is smaller than the calculated maximum NOE, $\tau_e$ is not negligible and contributes significantly to the relaxation parameters. For molecules undergoing anisotropic motion, this criterion is not strictly applicable because the NOE is also $\theta$ dependent. However, for the molecular dimensions similar to those of the model of $(POG)_{10}$ (Figure 2), the value of NOE is not very sensitive to variations in $\theta$. For example, the NOE magnitude changes only by $\sim$2% for $\theta$ values between 70 and 90°. Therefore the relative values of the experimental and theoretical NOEs can still be used to judge whether $\tau_e$ is contributing to the spectral density function.

## RESULTS

### *Assignment of Resonances in $(POG)_{10}$ and T3-785*

Previous studies have shown that both $(POG)_{10}$ and T3-785 form stable triple helices in aqueous solution, with melting temperatures respectively of 60 and 25 °C (Li et al., 1993). Labeled $^{15}N$ residues were introduced into these two triplets, and specific NMR assignments were obtained (Li et al., 1993) and are used in the present dynamics studies. A brief summary of the assignments are presented here. In $(POG)_{10}$, the central glycine corresponding to residue 15 is labeled with $^{15}N$, and as seen in Figure 3A, only one cross-peak is detected in the $^1H$-$^{15}N$ correlation spectrum. This peptide is fully trimerized, with no monomer present at 10 °C, so the presence of only one cross-peak indicates that the three glycine residues of the three different chains in the molecule are equivalent in this repetitive peptide. In T3-785, the tripeptide unit Gly-Leu-Ala corresponding to residues 15–17 is labeled with $^{15}N$, and 12 well-resolved peaks are observed in the $^1H$-$^{15}N$ correlation spectrum (Figure 3B). Nine of the peaks arise from the triple-helical form of the peptide. Three peaks are seen for each residue type, one from each of the three chains. The residues of the three different chains are in chemically distinguishable environments, in contrast to the three glycines in the center of the peptide $(POG)_{10}$, which are in equivalent environments and give only one peak. The three remaining peaks are assigned to the Gly, Leu, and Ala in the monomer form. The assignments of T3-785 allow one to follow the dynamics of specific residues, in both the triple-helical and monomer form.

### *Measurement of $^{15}N$ Relaxation Parameters*

To investigate the backbone dynamics, $^{15}N$ relaxation data were acquired using inverse-detected $^1H$-$^{15}N$ NMR for the Gly in $(POG)_{10}$ and the nine triple-helical resonances and three monomer resonances for Gly-Leu-Ala in peptide T3-785 (Figure 4). The $T_1$ relaxation curves for the $^{15}N$-labeled glycine in $(POG)_{10}$ and the labeled glycines in T3-785 are shown in Figure 4a. For T3-785, a representative glycine resonance is chosen from chain 1 of the triple helix, and the glycine from the single-chain monomer is plotted as well. Figure 4b shows the $T_2$ relaxation curves for the same glycine resonances as in Figure 4a. All the relaxation curves can be fit with single exponentials. The best fit values of the relaxation rates $R_1$ and $R_2$ for residues in both peptides are presented along with the $R_2/R_1$ ratio in Table I. The measured heteronuclear NOE for each residue is also listed.

For the trimer form of T3-785, the $R_1$ and $R_2$ relaxation rates of Gly, Leu, and Ala in the three different chains are similar in magnitude. In addition, the NOE values are greater than 0.72 for all but one residue. Therefore, in the analysis, the relaxation parameters for each labeled residue are averaged over the three chains. Statistical analysis indicates that the averaged $R_2/R_1$ ratio for Ala is higher than those for Gly and Leu and that the Gly and Leu values are not distinguishable (Table I). Therefore, for further analysis of the data, an average $R_2/R_1$ of 7.74 is determined for Gly and Leu and an average $R_2/R_1$ of 8.44 is used for Ala.

The relaxation parameters for the monomer form of T3-785 show striking differences from those for the trimer form. In particular, the $T_2$ relaxation rates for the monomer residues are about 7 times smaller than the $T_2$'s for the trimer conformation, and the NOEs in the monomer form are negative compared to the large positive NOEs in the trimer form.

The relaxation rates for the Gly in $(POG)_{10}$ (all trimer) were in the same general range as the values for the T3-785 trimer, but the $R_2$ value was higher for $(POG)_{10}$ and resulted in a higher $R_2/R_1$ ratio.

### *Analysis of the Relaxation Parameters for $(POG)_{10}$ and T3-785*

*Form of the Spectral Density Function for an Anisotropic Triple Helix.* The relaxation data can be interpreted for each

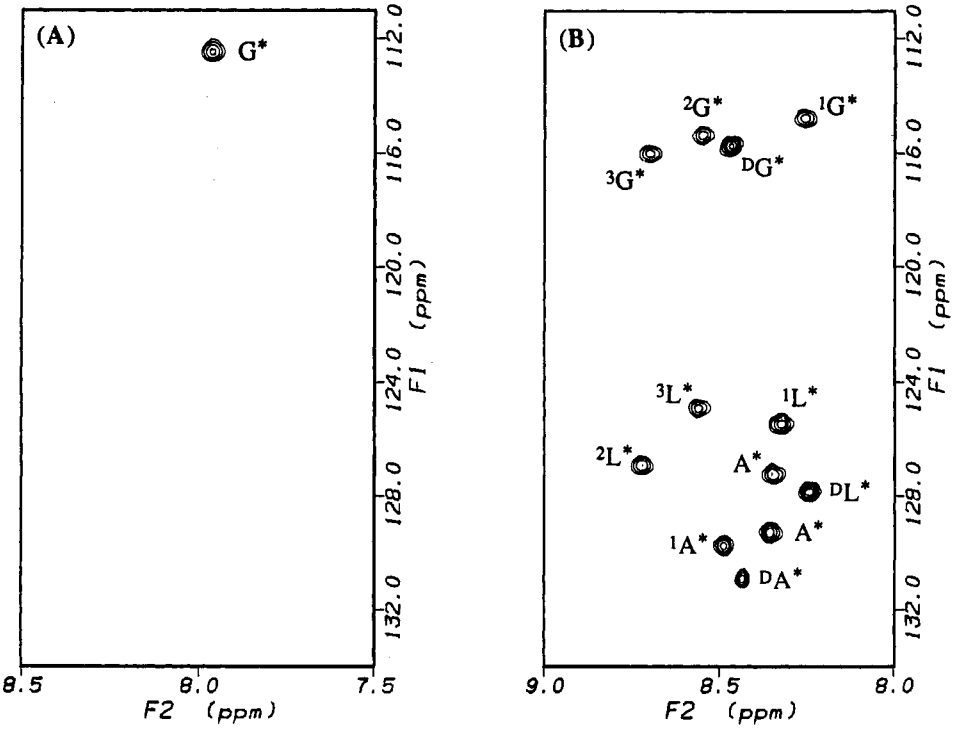


FIGURE 3: HMQC spectra in 90% $H_2O$/10% $D_2O$ solution at 10 °C, pH 2.6, for (A) $(POG)_{10}$ and (B) T3-785. The assignments of the $^1H$-$^{15}N$ correlation peaks of the three labeled residues G*, L*, and A* in T3-785 are shown (Li et al., 1993). The resonances from the three chains of the triple helix are designated with the chain number 1, 2, or 3 in the superscript, and the resonances from the monomer form are designated with a D superscript. Two of the Ala residues in the trimer form cannot be assigned to specific chains due to resonance overlap.

residue in terms of motional parameters once an appropriate spectral density function is chosen and the effect of chemical exchange on the $T_2$ relaxation is determined. As discussed in the theory section, for anisotropic overall motion, the $R_2/R_1$ ratio differs from residue to residue and therefore cannot easily be used to judge the effect of chemical exchange and internal motion. However, the NOE values are still useful in choosing the form of the spectral density function. To consider the magnitude of the NOE for the triple-helical peptides, the molecular dimensions from the fiber diffraction model of the triple-helical peptide ($L$ = 93 Å, $b$ = 13 Å) and a range of angle $\theta$ for the glycine N–H bond vector (70° < $\theta$ < 90°) (see next) have been used to calculate a theoretical maximum NOE of 0.72–0.74. The observed NOEs for residues in $(POG)_{10}$ and T3-785 trimer are all greater than or close to these values within the experimental error, which suggests that the contribution from the effective correlation time of the internal motion to the relaxation processes is negligible ($\tau_e$ = 0). To evaluate the contribution of conformational averaging ($R_{ex}$) to the $T_2$ relaxation, experimental data independent of the relaxation measurements needs to be used. For T3-785, according to the hydrogen–deuterium exchange rates reported in the next section and the estimated refolding rate of the molecule based on CD measurements (D. Siegel, M.H.L., B.B., and J.B., unpublished results), the calculated rate of trimer to monomer interconversion is approximately 1.6 × $10^{-5}$ $s^{-1}$. Compared to the observed $R_2$ relaxation rate of ~13.5 $s^{-1}$, the rate of chemical exchange is too slow to affect the $T_2$ relaxation. For $(POG)_{10}$, there is no monomer–trimer interconversion on the basis of either NMR (Li et al., 1993) or equilibrium sedimentation results (Long et al., 1993). Therefore, to analyze the relaxation parameters for $(POG)_{10}$ and T3-785, the simplified form of the spectral density function shown in eq 8 is used and the exchange term is excluded from the $T_2$ relaxation.

*Determination of Overall Motional Parameters ($L$, $b$, and $\theta$) and Order Parameter $S^2$ for Triple Helical Peptides.* The relaxation parameters $T_1$ and $T_2$ and the NOE are a function of the spectral density function which depends on $S^2$, the order parameter for the internal motion; $L$ and $b$, the dimensions of the molecule; and $\theta$, the angle between the N–H vector and the major axis of the molecule. To calculate the order parameters $S^2$, first the overall motion characterized by the parameters $L$, $b$, and $\theta$ needs to be determined. In the present case, these motional parameters are related directly to the $R_2/R_1$ ratio. Since $L$ and $b$ must be the same for a given peptide, the variation in the $R_2/R_1$ ratio for the Ala and Gly/Leu residues in T3-785 must represent differences in $\theta$ (Figure 5).

Since there is no unique solution for $L$, $b$, and $\theta$ for a particular $R_2/R_1$ ratio, overall motional parameters are chosen to be consistent with known triple-helix data. A range of valid $L$, $b$, and $\theta$ values are selected on the basis of consistency with the fiber diffraction data: 10 Å < $b$ < 16 Å, 80 Å < $L$ < 94 Å, and 70° < $\theta$ < 90°. For T3-785, when the $\theta$ values for both Ala and Gly/Leu are simultaneously restrained to be in the range 70–90°, a smaller range of $L$ and $b$ values become available on the basis of the experimental $R_2/R_1$ ratios, as seen in Figure 5. The family of dimensions that are consistent with the experimental data is $b$ = 14.5 Å with $L$ = 90.5–92 Å up to $b$ = 15.5 Å with $L$ = 86 Å. The ranges of valid $L$ values depend on the chosen $b$ values.

To give an example of the value of the order parameter $S^2$, specific $b$ (=14.5 Å) with $L$ (=91 Å) values are chosen within the valid range. For these $b$ and $L$ values, the experimental $R_2/R_1$ ratios for Ala and Gly/Leu residues correspond to $\theta_{Ala}$ = 85° and $\theta_{Gly/Leu}$ = 72°. Using these values, the order parameters for each labeled residue can be calculated from eqs 6–8 and the measured $T_1$ or $T_2$ values (Table II). Selection of different $L$ and $b$ values in the valid range gives similar

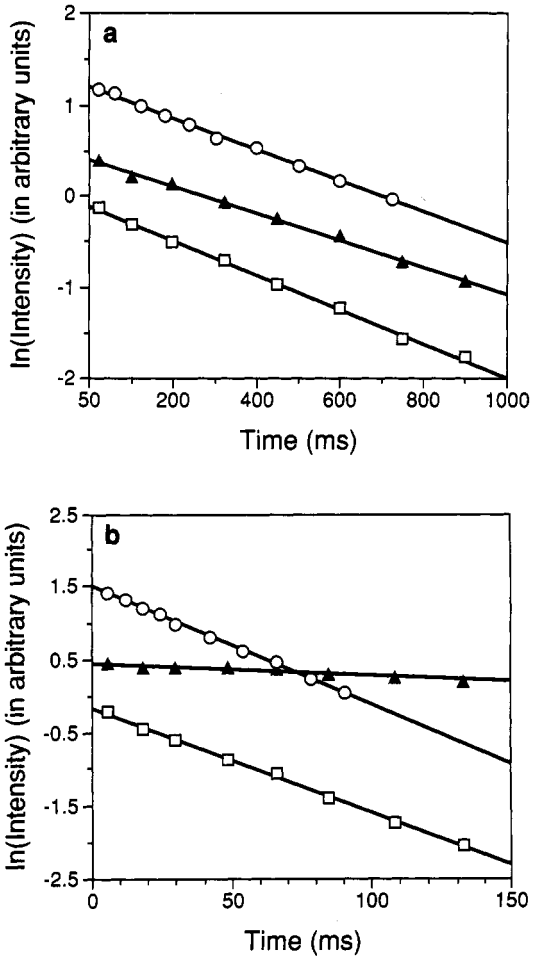


FIGURE 4: $^{15}N$ $T_1$ (a) and $T_2$ (b) relaxation decay curves at 10 °C: (○) the central glycine in $(POG)_{10}$; (□) a glycine residue in the trimer form of T3-785 ($^1$Gly*); (▲) the glycine residue in the monomer form of T3-785.

results for $S^2$, indicating that $S^2$ is not very sensitive to small differences in the dimensions of the molecule.

Order parameters for $(POG)_{10}$ were determined by selecting a specific $\theta$ and then calculating the order parameter for given molecular dimensions that satisfy the experimental data. Two different values of $\theta$ were used; one, $\theta = 85°$, was chosen on the basis of the fiber diffraction model, and the second one, $\theta = 72°$, was chosen from the calculation for T3-785. When $\theta = 85°$ (model), the valid ranges of $L$ and $b$ that satisfy the observed $R_2/R_1$ ratio are 14.5 Å $< b <$ 16 Å and 87.5 Å $< L <$ 94 Å. The order parameter $S^2$ calculated for the selected values of $b$ = 15.5 Å and $L$ = 89.7 Å gave a value of 0.82 (obtained by using eqs 6–8 and the $T_1$ or $T_2$ value). When $\theta = 72°$ (as found for Gly in T3-785), the valid ranges are 15.2 Å $< b <$ 16 Å and 89.5 Å $< L <$ 94 Å and selected values of $b$ = 15.5 and $L$ = 92.5 Å gave an order parameter of $S^2$ = 0.88. It is interesting to note that the calculated order parameter is quite sensitive to the angle $\theta$.

*Analysis of the T3-785 Monomer.* In contrast to those of the trimer, the relaxation parameters of the monomer resonances are analyzed on the basis of an isotropic model. Since our studies are on the backbone of central residues and the shape of the molecule is unknown, the simplest possible assumption is made and the motion is assumed to be isotropic. In the monomer case, the long $T_2$'s and the negative NOE values (Table I) suggest that the contribution of $\tau_e$ to the relaxation processes cannot be neglected and therefore the spectral density function shown in eq 4 is used in the analysis. Possible conformational exchange between different monomers is not considered due to the limited amount of experimental data. To obtain $S^2$, $\tau_e$, and the effective overall correlation time, $\tau_c$, for the three different residues in the monomer form, the following $\chi^2$ function is minimized:

$$\chi^2 = \sum_{i=1}^{n}\left[\frac{(R_{1obs} - R_{1cal})^2}{\sigma_1^2} + \frac{(R_{2obs} - R_{2cal})^2}{\sigma_2^2} + \frac{(NOE_{obs} - NOE_{cal})^2}{\sigma_{NOE}^2}\right] \quad (9)$$

where the subscript "obs" represents the measured relaxation values and the subscript "cal" represents the values calculated using eqs 1–4; the $\sigma_i$'s are the standard deviations obtained from repeated independent measurements; and the sum runs over the three labeled resonances in T3-785. In the minimization procedure, to find the overall correlation time $\tau_c$, a grid search is performed in the range of 0.2–5 ns with a step of 0.1 ns. For a given $\tau_c$, $S^2$ and $\tau_e$ are used as the adjustable parameters in the minimization. The $\tau_c$, $S^2$, and $\tau_e$ values which give the smallest $\chi^2$ are taken as the overall correlation time of the monomer and the parameters representing the internal motion of each labeled residue. The order parameters and the effective correlation times for the internal motion of the monomer form are listed in Table III.

### *Hydrogen-Exchange Measurements for $(POG)_{10}$ and T3-785*

The amide hydrogen exchange rates for each of the labeled residues in $(POG)_{10}$ and T3-785 were determined from $^1$H-$^{15}$N HMQC experiments at 10 °C, and the rates of exchange are listed in Table IV.

For the peptide T3-785, hydrogen-exchange rates were obtained for the 12 resonances at 10 °C, pH 3.6. The amide protons for the three residues in the monomer conformation exchange very rapidly, with glycine exchanging at a rate that is about 2 times faster than those of Leu and Ala. The amide protons in the trimer conformation exchange much more slowly than those in the monomer form. In the triple-helical conformation, the hydrogen-exchange rate is dependent on the position in a tripeptide unit. The exchange rates for the glycine and the leucine residues are slow and very similar to each other. However, the exchange rates for the alanine residues at the Y position are 14 times faster than those of the glycine and leucine. Protection factors, defined as the rate of exchange of the monomer divided by the rate of exchange of the trimer, are listed in Table IV. Hydrogen-exchange experiments were also performed at 18 °C and show trends very similar to those at 10 °C, although the overall rates were faster (data not shown).

For the single glycine residue in $(POG)_{10}$, no noticeable decrease of the amide proton intensity was observed within 24 h of sample dissolution at 10 °C and pH 3.6. The hydrogen-exchange experiment was performed at 18 °C, and the exchange rate was still too slow to be measured within the experimental time. An upper limit for the rate is calculated and listed in Table IV, assuming a 1% decrease in the intensity after 42 h. The intrinsic exchange rate for the Gly predicted for the random-coil form of the peptide, taking into account pH, temperature, and sequence effects, is calculated to be 4.5 $\times 10^{-2}$ min$^{-1}$ (Molday et al., 1972; Jeng & Englander, 1991). A lower limit for the protection factor based on the upper limit for the exchange rate is given in Table IV.

Table I: Measured Relaxation Parameters for the Labeled Residues in $(POG)_{10}$ and T3-785 at 10 °C

| residue | $R_1$ ($s^{-1}$) | $R_2$ ($s^{-1}$) | NOE | $R_2/R_1$ | $R_2/R_1$ av (grouping)[a] |
|---|---|---|---|---|---|
| | | | T3-785 Trimer | | |
| $^1$Gly* | 1.83 ± 0.07 | 14.0 ± 0.3 | 0.76 ± 0.03 | 7.68 ± 0.35 | |
| $^2$Gly* | 1.82 ± 0.10 | 14.0 ± 0.6 | 0.80 ± 0.05 | 7.67 ± 0.54 | 7.64 ± 0.06 (A) |
| $^3$Gly* | 1.81 ± 0.06 | 13.7 ± 0.3 | 0.72 ± 0.05 | 7.57 ± 0.28 | |
| $^1$Leu* | 1.66 ± 0.08 | 13.3 ± 0.1 | 0.74 ± 0.08 | 7.99 ± 0.37 | |
| $^2$Leu* | 1.73 ± 0.08 | 12.9 ± 0.2 | 0.77 ± 0.02 | 7.48 ± 0.39 | 7.83 ± 0.30 (A) |
| $^3$Leu* | 1.64 ± 0.05 | 13.2 ± 0.6 | 0.74 ± 0.04 | 8.02 ± 0.42 | |
| $^1$Ala* | 1.60 ± 0.01 | 14.2 ± 0.8 | 0.72 ± 0.04 | 8.91 ± 0.49 | |
| Ala* | 1.62 ± 0.08 | 13.5 ± 0.3 | 0.74 ± 0.06 | 8.33 ± 0.47 | 8.44 ± 0.42 (B) |
| Ala* | 1.60 ± 0.04 | 12.9 ± 0.5 | 0.68 ± 0.08 | 8.09 ± 0.38 | |
| | | | T3-785 Monomer | | |
| $^D$Gly* | 1.45 ± 0.02 | 1.59 ± 0.04 | −0.59 ± 0.15 | 1.09 ± 0.03 | |
| $^D$Leu* | 1.50 ± 0.06 | 2.21 ± 0.00 | −0.50 ± 0.06 | 1.47 ± 0.06 | |
| $^D$Ala* | 1.36 ± 0.02 | 1.52 ± 0.25 | −0.68 ± 0.01 | 1.12 ± 0.23 | |
| | | | $(POG)_{10}$ Trimer | | |
| Gly* | 1.72 ± 0.09 | 15.9 ± 0.8 | 0.81 ± 0.03 | 9.24 ± 0.67 | |

[a] A one-way analysis of variance (ANOVA) (Cody & Smith, 1987) was performed for the nine different $R_2/R_1$ values (two data sets) of the T3-785 trimer, to test the null hypothesis that the means for Gly, Leu, and Ala are indistinguishable. This hypothesis was rejected at a 0.05 level, and a Duncan multiple range test indicated that Gly and Leu $R_2/R_1$ values are not statistically different ($p < 0.05$ and letter grouping A) but that Ala had $R_2/R_1$ values significantly higher than both Gly and Leu (group B).

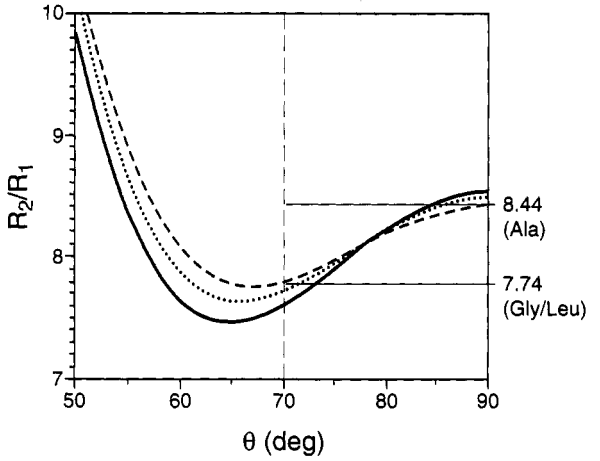


FIGURE 5: Calculated $R_2/R_1$ ratio as a function of $\theta$ angle using the cylinder model with three different lengths ($L$) and widths ($b$): (—) $L = 91.0$ Å, $b = 14.5$ Å; (···) $L = 88.5$ Å, $b = 15.0$ Å; (- - -) $L = 86.0$ Å, $b = 15.5$ Å. The experimental $R_2/R_1$ ratios for the Ala and Gly/Leu in the peptide T3-785 are marked by solid horizontal lines. When $\theta$ is confined between 70 and 90° (indicated by a vertical dashed line), only a few values of $b$ and $L$ in the range defined for triple-helical peptides generate curves intersecting both experimental $R_2/R_1$ ratios. These values are taken as the valid molecular dimensions for the peptide T3-785. For a given set of valid $b$ and $L$, the $\theta$ angles for the Ala and Gly/Leu are determined from the points of intersection.

Table II: Molecular Dimensions and Averaged Order Parameters for Each Labeled Residue in $(POG)_{10}$ and T3-785 at 10 °C

| residue | $L$ (Å) | $b$ (Å) | $\theta$ (deg) | $S^2$ |
|---|---|---|---|---|
| | | T3-785 Trimer | | |
| Gly* | 91.0 | 14.5 | 72 | 0.85 ± 0.03 |
| Leu* | 91.0 | 14.5 | 72 | 0.79 ± 0.03 |
| Ala* | 91.0 | 14.5 | 85 | 0.72 ± 0.04 |
| | | $(POG)_{10}$ | | |
| Gly* | 92.5 | 15.5 | 72[a] | 0.88 ± 0.04 |
| | 89.7 | 15.5 | 85[b] | 0.82 ± 0.04 |

[a] Chosen from the calculation for T3-785. [b] Chosen on the basis of the fiber diffraction model.

## DISCUSSION

The backbone dynamics of specific residues in the triple-helical peptides $(POG)_{10}$ and T3-785 were studied. $(POG)_{10}$ is a peptide that contains the highest possible imino acid content (67%), while the peptide T3-785 is a 30-mer containing an imino acid poor central region surrounded by POG caps. Different time scales of molecular motion are probed using $^{15}N$ relaxation measurements and hydrogen exchange. The former probes molecular motions that are similar to or faster than the overall rotational diffusion of the molecule (ps–ns), and the latter reflects slower motions probably on the time scale of milliseconds or longer. A comparison of the backbone dynamics of the two peptides on these different time scales may lead to information about how conformational flexibility is related to collagen function and recognition.

An anisotropic treatment of the relaxation data of $(POG)_{10}$ and T3-785 is dictated by the rodlike dimensions predicted

Table III: Order Parameters and Effective Correlation Times of the Monomer Residues of T3-785 at 10 °C[a]

| residue | $S^2$ | $\tau_e$ (ps) |
|---|---|---|
| Gly* | 0.39 | 111 |
| Leu* | 0.54 | 130 |
| Ala* | 0.39 | 97 |

[a] The overall rotational correlation time is determined to be 1.6 ns.

Table IV: Hydrogen-Exchange Rates and Protection Factors ($P$) for Each Labeled Residue in $(POG)_{10}$ and T3-785 at 10 °C, pH 3.6

| residue | $k_{exch}$ ($10^{-4}$ $min^{-1}$) | $\bar{k}_{exch}$ ($10^{-4}$ $min^{-1}$) | $P$ |
|---|---|---|---|
| | T3-785 Trimer | | |
| $^1$Gly* | 0.6 | | |
| $^2$Gly* | 0.5 | 0.5[a] | 1077[b] |
| $^3$Gly* | 0.5 | | |
| $^1$Leu* | 0.7 | | |
| $^2$Leu* | 0.7 | 0.8[a] | 418[b] |
| $^3$Leu* | 1.1 | | |
| $^1$Ala* | 10.6 | | |
| Ala* | 8.9 | 9.6[a] | 34[b] |
| Ala* | 9.4 | | |
| | T3-785 Monomer | | |
| $^D$Gly* | 571 | | |
| $^D$Leu* | 348 | | |
| $^D$Ala* | 329 | | |
| | $(POG)_{10}$ | | |
| Gly* | <0.04 | | >$10^4$ [c] |

[a] $\bar{k}_{exch}$ is the average rate for three residues. [b] $P$ is defined as $P = k_{exch}(monomer)/\bar{k}_{exch}(trimer)$. [c] $P$ is defined as $P = k_{int}/k_{exch}(trimer)$, where the intrinsic exchange rate ($k_{int}$) is calculated at pH 3.6 and 10 °C including the nearest neighbor effect (Molday et al., 1972; Jeng & Englander, 1991).

for these peptides on the basis of fiber diffraction data (Fraser et al., 1979) as well as NMR experiments (Torchia et al., 1975; Li et al., 1993). In anisotropic systems, the overall motional parameters can vary from one residue to the next, as the angle $\theta$ of the N–H vectors with respect to the major axis of the molecule can vary for different residues. In the case of isotropic motion, where the overall motional parameter is the same for all residues, the $R_2/R_1$ ratio plays a crucial role in determining the contribution of chemical exchange ($R_{ex}$) to the relaxation processes and the time scale of the internal motion. Because of the angular dependence of the overall motion, the $R_2/R_1$ ratio can no longer be used straightforwardly for the same purpose in the anisotropic case. In the present study of the triple-helical peptides, the magnitudes of the $^1$H-$^{15}$N NOE and hydrogen exchange have been used to estimate the effects of these factors on the relaxation parameters. The effect of chemical exchange is ignored because the rate is too slow, as estimated from the hydrogen-exchange and refolding experiments. The effective correlation time of internal motion ($\tau_e$) is also neglected on the basis of the observed large $^1$H-$^{15}$N NOE value. Under these conditions, the internal motion decreases $R_1$ and $R_2$ by the same proportion and the $R_2/R_1$ ratio is only a function of the overall motional parameters. In the anisotropic case, a few sets of molecular dimensions and angular parameters ($L$, $b$, and $\theta$) which agree with the triple-helix model can satisfy an observed $R_2/R_1$ ratio, in contrast to the isotropic case, where the $R_2/R_1$ ratio can uniquely determine the overall motion of the molecule (characterized by $\tau_c$). Fortunately, within the set of the reasonable overall motional parameters, the calculated order parameters $S^2$ from the relaxation data do not vary significantly.

The order parameter $S^2$ of the central-labeled glycine in $(POG)_{10}$ is calculated to be in the range 0.82–0.88, which is comparable to values observed in the structured regions of globular proteins (Kay et al., 1989; Clore et al., 1990; Stone et al., 1992). The magnitude of the order parameter suggests that the backbone of $(POG)_{10}$ is quite rigid. This is consistent with the high degree of order and stability of the molecule. The Gly residue in $(POG)_{10}$ is in the most imino acid rich environment possible, with glycine tightly packed in the center of the helix and hydrogen bonded to the neighboring chain. The glycine at the same position in the triple-helical form of T3-785 has an order parameter (0.85) very similar to that of the $(POG)_{10}$. This glycine residue in T3-785 resides in one of the most imino acid poor regions of type III collagen, and it has been suggested that regions with low imino acid content may have increased flexibility or alternative conformations (Ramachandran, 1967; Fields, 1991). Yet, the similarity of the order parameter suggests that the backbone mobility of the triple-helical peptides on the picosecond time scale is not sensitive to the sequence composition and that the amplitude of the internal motion for the Gly in the imino acid poor environment is similar to that of the Gly in the stabilizing Pro-Hyp-Gly environment.

Within T3-785, comparison of the order parameters for the Gly, X, and Y positions of a given triplet can clarify whether there is more flexibility for residues in the X and Y positions than for the closely packed glycines. The results indicate that all three residues have a high degree of rigidity (the order parameters for Gly, Leu, and Ala are 0.85, 0.79, and 0.72, respectively). However, there are small variations in the order parameters, suggesting that Gly may be the most rigid, followed by the Leu in the X position and Ala in the Y position.

T3-785 is largely in a triple helical form at low temperature, but a small amount of monomer is also present in solution (Li et al., 1993; E. Braswell, personal communication). The order parameters for the three residues in the monomer form range from 0.39 to 0.54, with Leu showing the highest order parameter. The small order parameters reflect the high backbone mobility of the molecule, which is consistent with the flexible nature of the monomer form. Previous studies also indicate high mobility in the monomer form of peptides with $(X\text{-}Y\text{-}Gly)_n$ sequences, with differences in mobility between the central and terminal residues (Torchia et al., 1975; Daragan & Mayo, 1992).

Backbone dynamics were monitored on a slower time scale by measuring the hydrogen-exchange rates of individual amide protons of $^{15}$N-labeled residues in $(POG)_{10}$ and T3-785. The amide protons of the glycine in the center of $(POG)_{10}$ do not exchange even after 42 h, in agreement with the very slow exchange measured previously for collagen and other triple-helical peptides (von Hippel, 1967; Segal, 1969; Privalov et al., 1979). The current model for $(POG)_{10}$, based on fiber diffraction data, has the glycyl NH group hydrogen-bonded to the carbonyl oxygen of the prolyl residue in a neighboring chain, with the amide group well packed in the middle of the triple helix (Fraser et al., 1979) (see Figure 1). The hydrogen bonding and central location are consistent with the observed extremely slow exchange rate.

The hydrogen-exchange rates were also measured for the $^{15}$N-enriched Gly, Leu, and Ala residues in the center of the peptide T3-785 in both the trimer and monomer forms. The amide groups of all three residues exchange very quickly in the monomer form and are similar to rates (within a factor of 2) expected from the theoretical calculation of the random-coil rate for this peptide (Molday et al., 1972; Jeng & Englander, 1991). The exchange rates for Gly, Leu, and Ala in the triple helix are much slower. Comparison of the exchange of the glycyl NH of $(POG)_{10}$ with the glycyl NH of T3-785 indicates a faster exchange rate for the latter peptide. This indicates that the glycyl NH exchange rate is dependent on the X and Y residues in the $(X\text{-}Y\text{-}Gly)_n$ sequence of the peptide and that the peptide containing a lower imino acid content gives the faster rate. The difference in rate is expressed as, at least, a 10-fold difference in protection factor between the glycine NH's of the two peptides. The difference in protection factors can be related to a difference in the stability of the peptides (Englander & Kallenbach, 1984; Roder, 1989), and in this case, $(POG)_{10}$ with the larger protection factor has a $\Delta G = -22.9$ kcal/mol compared with peptide T3-785, which has a $\Delta G = -8.2$ kcal/mol (D. Siegel, M.H.L., B.B., & J.B., unpublished result).

Within the single Gly-Leu-Ala triplet of T3-785, the hydrogen-exchange rates and protection factors are not uniform. Gly and Leu have similar exchange rates and are more protected from exchange than Ala. However, even the Ala is significantly more protected from exchange than would be expected for a disordered form, as indicated by the protection factor of 30. The different rates of exchange may arise from differential solvent accessibility and/or hydrogen bonding. Although a model with only one hydrogen bond per tripeptide is the only possible one for $(POG)_{10}$ and has been supported by a number of lines of evidence (Katz, 1970; Fraser & MacRae, 1973), a model with two hydrogen bonds per tripeptide has been proposed for X-Y-Gly sequences where X is not an imino acid (Ramachandran, 1988). In the one-bond model, amide groups in the X and Y positions are pointing out to the solvent, leading to the expectation that amides in

the X and Y positions should exchange much more rapidly than the Gly. The observation that Gly and Leu have rather similar exchange rates is difficult to reconcile with this model. The results are more consistent with a two-bonded model in which the amide group of the X residue along with the Gly points inward, making a hydrogen bond with a carbonyl in an adjacent chain either directly or indirectly through a water bridge. Our results are consistent with tritium-exchange studies on soluble collagens which showed that about one amide hydrogen per triplet exchanges at the fast rates expected for the free peptide, while the remaining amide hydrogens exchange much more slowly (Yee et al., 1974). The observation that the protection factor for Ala in the triple helix is higher than that for an unordered chain indicates that the alanyl amide groups are likely to be engaged in some hydrogen-bonding interaction as well, possibly to tightly bound water molecules on the surface of the triple helix (Tuchsen & Woodward, 1985).

Backbone dynamics of triple-helical peptides were obtained to determine whether there are sequence-dependent motional properties and to clarify whether flexibility is important in specifying functional regions along collagen. By both hydrogen-exchange methods and relaxation measurements, the residue in the Y position (Ala) of T3-785 appears to be more mobile than residues in the Gly and X positions of the $(X\text{-}Y\text{-}Gly)_n$ repeating sequence. Comparisons of the relative mobilities of Gly in $(POG)_{10}$ and T3-785 give different results, depending on the method used. The motional properties on the picosecond time scale obtained from $^{15}N$ relaxation measurements are rather uniform, with little difference between the internal motional parameters of the Gly residues in $(POG)_{10}$ and T3-785. This suggests that backbone molecular motion on a fast time scale is sequence independent and, therefore, may not be important for recognition of specific triple-helical regions. In contrast, the hydrogen-exchange results suggest that on a slower time frame, probably milliseconds or longer, the backbone motion of the triple helix is sequence dependent with faster exchange for the glycine of T3-785 than for the glycine of $(POG)_{10}$. The sequence-dependent differences in the hydrogen-exchange rates are probably related to differences in the stability of the two peptides and may have important consequences for the binding and recognition of specific collagen sequences.

## ACKNOWLEDGMENT

We thank Yanbo Ding for carrying out the statistical analysis and Patrice Gryary for advice on statistics.

## REFERENCES

Abragam, A. (1961) *Principles of Nuclear Magnetism*, Oxford University Press, London.

Barbato, G., Ikura, M., Kay, L. E., Pastor, R. W., & Bax, A. (1992) *Biochemistry 31*, 5269–5278.

Bax, A., Griffey, R. H., Hawkins, B. L. (1983) *J. Magn. Reson. 55*, 301–315.

Berglund, H., Kovacs, H., Dahlman-Wright, K., Gustafsson, J., & Hard, T. (1992) *Biochemistry 31*, 12001–12011.

Brodsky-Doyle, B., Leonard, K. R., & Reid, K. B. (1976) *Biochem. J. 159*, 279–286.

Broersma, S. (1960) *J. Chem. Phys. 32*, 1626–1631.

Clore, G. M., Driscoll, P. C., Wingfield, P. T., & Gronenborn, A. M. (1990) *Biochemistry 29*, 7387–7401.

Cody, R. P., & Smith, J. K. (1987) *Applied Statistics and the SAS Programming Language*, 2nd ed., Elsevier Science Publishing Co., New York.

Constantine, K. L., Friedrichs, M. S., Goldfarb, V., Jeffrey, P. D., Sheriff, S., & Mueller, L. (1993) *Proteins: Struct. Funct. Genet. 15*, 290–311.

Daragan, V. A., & Mayo, K. H. (1992) *J. Am. Chem. Soc. 114*, 4326–4331.

Dolz, R., & Heidemann, E. (1986) *Biopolymers 25*, 1069–1080.

Englander, S. W., & Kallenbach, N. R. (1984) *Q. Rev. Biophys. 16*, 521–655.

Fields, G. B. (1991) *J. Theor. Biol. 153*, 585–602.

Fietzek, P. P., & Kuhn, K. (1975) *Mol. Cell. Biochem. 8*, 141–157.

Fraser, R. D. B., MacRae, T. P. (1973) *Conformation in Fibrous Proteins*, Academic Press, New York.

Fraser, R. D. B., MacRae, T. P., & Suzuki, E. (1979) *J. Mol. Biol. 129*, 463–481.

Guidry, C., Miller, E. J., & Hook, M. (1990) *J. Biol. Chem. 265*, 19230–19236.

Jelinski, L. W., & Torchia, D. A. (1980) *J. Mol. Biol. 138*, 255–272.

Jelinski, L. W., Sullivan, C. E., Batchelder, L. S., & Torchia, D. A. (1980) *Biophys. J. 32*, 515–529.

Jeng, M.-F., & Englander, S. W. (1991) *J. Mol. Biol. 221*, 1045–1061.

Katz, E. P. (1970) *Biopolymers 9*, 745–748.

Kay, L. E., Torchia, D. A., & Bax, A. (1989) *Biochemistry 28*, 8972–8979.

Kay, L. E., Nicholson, L. K., Delaglio, F., Bax, A., & Torchia, D. A. (1992) *J. Magn. Reson. 97*, 359–375.

Kirchhofer, D., Languino, L. R., Rouslahti, E., & Pierschbacher, M. D. (1990) *J. Biol. Chem. 265*, 615–618.

Kitchen, D. B., Hirata, F., Westbrook, J. D., Levy, R. M., Kofke, D., & Yarmush, M. (1990) *J. Comput. Chem. 11*, 1169–1180.

Kodama, T., Freeman, M., Rohrer, L., Zabrecky, P. M., & Krieger, M. (1990) *Nature 343*, 531–535.

Kordel, J., Skelton, N. J., Akke, M., Palmer, A. G., III, & Chazin, W. J. (1992) *Biochemistry 31*, 4856–4866.

Lamb, H. (1945) *Hydrodynamics*, Dover Publications, New York.

Li, M., Fan, P., Brodsky, B., & Baum, J. (1993) *Biochemistry 32*, 7377–7387.

Linsenmayer, T. (1991) in *Cell Biology of Extracellular Matrix* (Hay, E. D., Ed.) pp 7–44, Plenum Press, New York.

Lipari, G., & Szabo, A. (1982) *J. Am. Chem. Soc. 104*, 4546–4559.

Long, C. G., Braswell, E., Zhu, D., Apigo, J., Baum, J., & Brodsky, B. (1993) *Biochemistry*, in press.

Marion, D., & Wuthrich, K. (1983) *Biochem. Biophys. Res. Commun. 113*, 967–974.

Miller, E. J. (1984) in *Extracellular Matrix Biochemistry* (Piez, K. A., & Reddi, A. H., Eds.) pp 41–82, Elsevier, New York.

Miller, E. J., Finch, J. E., Jr., Chung, E., Butler, W. T., & Robertson, P. B. (1976) *Arch. Biochem. Biophys. 173*, 631–637.

Molday, R. S., Englander, S. W., & Kallen, R. G. (1972) *Biochemistry 11*, 150–158.

Mueller, L. (1979) *J. Am. Chem. Soc. 101*, 4481–4484.

Nemethy, G., & Scherage, H. A. (1984) *Biopolymers 23*, 2781–2799.

Nirmala, N. K., & Wagner, G. (1988) *J. Am. Chem. Soc. 110*, 7557–7558.

Palmer, A. G., III, Rance, M., & Wright, P. E. (1991) *J. Am. Chem. Soc. 113*, 4371–4380.

Palmer, A. G., III, Skelton, N. J., Chazin, W. J., Wright, P. E., & Rance, M. (1992) *Mol. Phys. 75*, 699–711.

Powers, R., Clore, G. M., Stahl, S. J., Wingfield, P. T., & Gronenborn, A. (1992) *Biochemistry 31*, 9150–9157.

Privalov, P. L., Tiktopulo, & Tischenko, V. M. (1979) *J. Mol. Biol. 127*, 203–216.

Ramachandran, G. N. (1967) in *Treatise on Collagen* (Ramachandran, G. N., Ed.) Vol. 1, pp 103–183, Academic Press, New York.

Ramachandran, G. N. (1988) *Int. J. Peptide Protein Res. 31*, 1–16.

Redfield, A. G., & Kunz, S. D. (1975) *J. Magn. Reson. 19*, 250–254.
Redfield, C., Boyd, J., Smith, L. J., Smith, R. A. G., & Dobson, C. M. (1992) *Biochemistry 31*, 10431–10437.
Rich, A., & Crick, F. H. C. (1961) *J. Mol. Biol. 3*, 483–506.
Roder, H. (1989) *Methods Enzymol. 176*, 446–472.
Ryhanen, L., Zaragoza, E. J., & Vitto, J. (1983) *Arch. Biochem. Biophys. 223*, 562–571.
Sarkar, S. K., Hiyama, Y., Niu, C. H., Young, P. E., Gerig, J. T., & Torchia, D. A. (1987) *Biochemistry 26*, 6793–6800.
Schneilder, D. M., Dellwo, M. J., & Wand, A. J. (1992) *Biochemistry 31*, 3645–3652.
Segal, D. M. (1969) *J. Mol. Biol. 43*, 497–517.
Seyer, J. M., Mainardi, C., & Kang, A. H. (1980) *Biochemistry 19*, 1583–1589.
Staatz, W. D., Fok, K. F., Zutter, M. M., Adams, S. P., Rodriguez, B. A., & Santoro, S. A. (1991) *J. Biol. Chem. 266*, 7363–7367.
Stone, M. J., Chandrasekhar, K., Holmgren, A., Wright, P. E., & Dyson, H. J. (1993) *Biochemistry 32*, 426–435.
Stone, M. J., Fairbrother, W. J., Palmer, A. G., III, Reizer, J., Saier, M. H., Jr., & Wright, P. E. (1992) *Biochemistry 31*, 4394–4406.
Torchia, D. A. (1982) *Methods Enzymol. 82*, 174–186.
Torchia, D. A., Lyerla, J. R., Jr., & Quattrone, A. J. (1975) *Biochemistry 14*, 887–900.
Tromp, G., Kuivaniemi, H., Shikata, H., & Prockop, D. J. (1989) *J. Biol. Chem. 264*, 1349–1352.
Tuchsen, E., & Woodward, C. (1985) *J. Mol. Biol. 185*, 421–430.
van der Rest, M., & Garrone, R. (1991) *FASEB J. 5*, 2814–2823.
von Hippel, P. H. (1967) in *Treatise on Collagen* (Ramachandran, G. N., Ed.) pp 253–338, Academic Press, New York.
Wagner, G. (1983) *Q. Rev. Biophys. 16*, 1–57.
Woessner, D. E. (1962) *J. Chem. Phys. 37*, 647–654.
Woodward, C. K., & Hilton, B. D. (1979) *Annu. Rev. Biophys. Bioeng. 8*, 99–127.
Yee, R. Y., Englander, S. W., & von Hippel, P. H. (1974) *J. Mol. Biol. 83*, 1–16.